8

Radiation parameterizations

8.1 Introduction

Radiation is the ultimate driver of atmospheric circulations, since radiation passes through the atmosphere and reaches the Earth's surface in amounts that are unequally distributed in space and time. This unequal energy distribution, due in part to the Earth's spherical shape, produces horizontal gradients in temperature, which produce atmospheric motions. Radiation not only determines the Earth's climate, but also plays a significant role in local energy budgets by providing the largest energy source terms. Radiation is unique among atmospheric processes since it can transport energy without a medium, yet it interacts with gases, liquids, and solids in very different ways.

Changes in the mean annual net radiation of a fraction of 1% can lead to significant changes in global climate when this change persists over a number of years. This highlights the importance of accurate radiation parameterizations to global climate models that are being used both to understand how increasing greenhouse gas concentrations affect future climate and to provide guidance to policy makers across the world. However, radiation also is important in the day-to-day weather events that influence our lives. Just think of a chilly fog-filled morning that breaks into a sunny and warm afternoon and the effects of radiation on the weather we experience become clear. Radiation is a key player in the atmosphere, both on very short and very long timescales. Thus, radiation needs to be parameterized accurately under a wide variety of atmospheric conditions.

Radiation parameterizations are intended to provide a fast and accurate method of determining the total radiative flux at any given location. These calculations provide both the total radiative flux at the ground surface, which is needed for the surface energy budget, and the vertical radiative flux divergence, which is used to calculate the radiative heating and cooling rates of a

given atmospheric volume. We know from Chapters 2 and 3 that the magnitude of the terms in the surface energy budget can set the stage for moist deep convection and are crucial to the formation of low-level clouds. In addition, the vertical radiative flux divergence can produce substantial cooling, particularly at the tops of clouds, which can have a strong dynamic effect on cloud evolution. While one can also use the total radiative flux to calculate the horizontal radiative flux divergence, this term is often neglected in numerical models owing to scaling arguments. Once the upward (F_U) and downward (F_D) radiative flux densities ($\mathrm{W\,m^{-2}}$) are determined, the heating rate for a given layer of the atmosphere is defined as

$$\frac{\partial T}{\partial t} = \frac{1}{\rho c_p} \frac{\partial}{\partial z} (F_D - F_U). \tag{8.1}$$

The challenge of radiation parameterizations is to find ways to calculate F_U and F_D efficiently and accurately. This is because global climate models (GCMs) have found that the radiation parameterization calculations can easily consume most of the computer resources needed for the model simulations. As is seen throughout this and the following chapter, we are still far from handling radiation well when clouds are present and some difficulties remain in clear skies as well.

The spectral distributions of solar and terrestrial irradiance received at sea level through a cloud and haze-free atmosphere (Fig. 8.1) indicate that several simplifications are possible for radiation parameterizations. First, the shortwave (solar) and longwave (terrestrial) portions of the spectra are distinct and, therefore, can be treated separately. Second, many of the gases that absorb either solar or longwave radiation (H_2O, CO_2, O_2, O_3, etc.) are associated with specific wavelength bands (Fig. 8.2). While there are some wavelength bands for which multiple gases absorb energy, the number of bands for which only a single gas is important is a fairly large fraction of the total.

Most parameterization schemes are either highly empirically driven approaches that use bulk expressions for gaseous absorption and clouds, or approaches that use two-stream or related approximations. Two-stream approximations attempt to represent the total radiative flux in two streams: one for the downward component and one for the upward component. Thus, many of the schemes available today either use bulk column properties to parameterize the shortwave and longwave contributions separately, or use a two-stream approach to calculate the shortwave and longwave contributions for both the upward and downward components. Before we discuss the specifics of various approaches to simplifying the radiation calculations, a few concepts are reviewed.
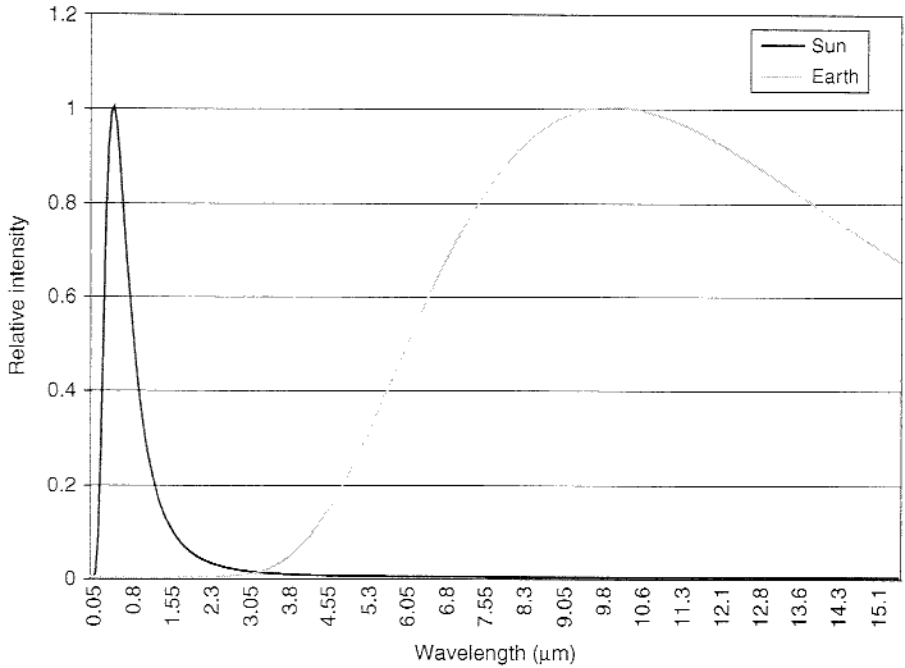
Figure 8.1. Radiative flux calculated using the Planck function and normalized to 1 as a function of wavelength for the sun ($T = 6000$ K, black line) and the Earth ($T = 290$ K, gray line). Note the lack of overlap between the two curves, which allows for the shortwave (sun) and longwave (Earth) components to be treated separately.
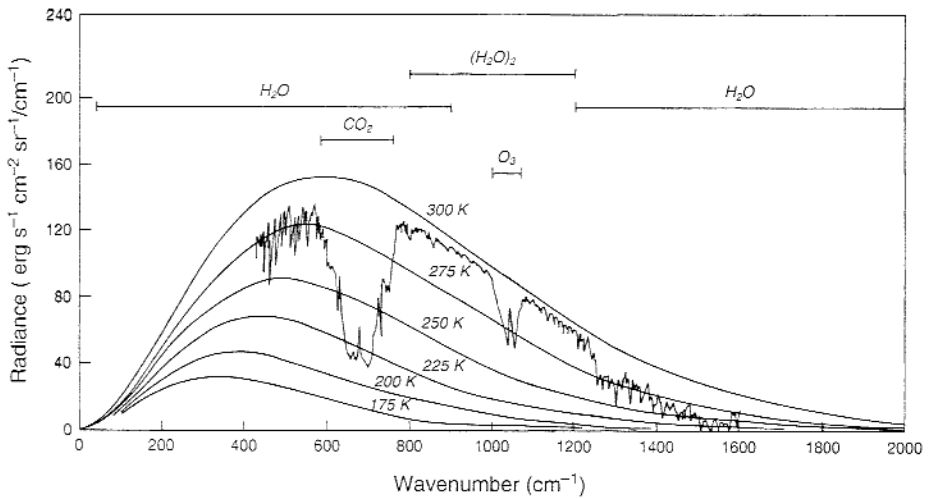

Figure 8.2. Terrestrial longwave spectra calculated for selected temperatures, with the various absorption bands indicated. Also shown is the actual emission spectrum taken by the Nimbus IV IRIS instrument near Guam on 27 April 1970. From Liou (1980), reprinted with permission from Elsevier.

8.2 Basic concepts

Electromagnetic radiation can be described as an ensemble of waves of varying wavelength that all travel through a vacuum at the same speed – the speed of light. The totality of all of these waves with different wavelengths represents the electromagnetic spectrum (see Wallace and Hobbs 1977; Liou 1980; Goody and Yung 1995). The human eye is sensitive to only a small wavelength band within this spectrum called visible light. But waves with both smaller (X-ray and ultraviolet) and longer (near-infrared, infrared, and microwave) wavelengths also are important to understanding the atmospheric energy budget. All materials with temperatures above absolute zero emit electromagnetic radiation continually.

The electromagnetic spectrum produced by a given source depends upon its composition and physical state. Solids and liquids produce a continuous electromagnetic spectrum, as illustrated by the smoothly varying curves in Fig. 8.2. as do incandescent gases under extremely high pressure such as the sun. However, luminous gases at low pressure, such as the polar aurora, produce spectra that consist of distinct lines. These lines occur because an isolated molecule can only emit and absorb energy in discrete units called photons, in contrast to the strongly interacting molecules found in liquids, solids, and gases at extreme pressure that together emit and absorb nearly all incident electromagnetic radiation. An isolated molecule can transition to a higher energy level by absorbing electromagnetic radiation, or can transition to a lower energy level by emitting electromagnetic radiation. But only discrete changes in energy are allowed. Since the energy of a photon of radiation depends upon its wavelength, the discrete nature of the various energy transitions in an isolated molecule leads to a spectrum of distinct absorption or emission lines that are very narrow and defined by the allowed changes in energy level, separated by gaps in the spectrum for which no absorption or emission is possible.

When a continuous electromagnetic spectrum, such as that produced by the sun, passes through cool gases, such as found in the atmosphere, the observed spectrum that reaches the ground is influenced by the selective absorption of radiation by the gas molecules encountered. These molecules absorb the electromagnetic radiation at distinct wavelengths, producing absorption lines in the spectrum. The resulting spectra show the continuous electromagnetic spectrum of the source interrupted by bands or lines that are a result of the selective absorption. The width and shape of these absorption lines are influenced by the atmospheric pressure and temperature through the effects of Doppler and pressure broadening (Liou 1980). Thus, the absorption lines

associated with the gases that constitute the atmosphere, with liquid water and ice from clouds, and with aerosols from natural and anthropogenic sources, are important to determining the amount of radiation that is transferred through the atmosphere and absorbed by it.

8.2.1 Blackbody radiation

As discussed thoroughly by Liou (1980), Planck made two assumptions for atomic oscillators in 1901 that led to the development of what is now called Planck's law. He first assumed that an oscillator can only have specific energies, i.e. that the energy is quantized. Second, he assumed that oscillators only radiate energy in discrete jumps or quanta. These assumptions led to the development of the Planck function B_ν

$$B_\nu(T) = \frac{2h\nu^3}{c^2(e^{h\nu/k_B T} - 1)}, \tag{8.2}$$

where ν is the frequency, T is the absolute temperature, k_B is Boltzmann's constant $(1.3806 \times 10^{-23}\,\mathrm{J\,K^{-1}})$, c is the velocity of light $(3.0 \times 10^8\,\mathrm{m\,s^{-1}})$, and h is the Planck constant $(6.6262 \times 10^{-34}\,\mathrm{J\,s})$. This can also be written in terms of wavelength $\lambda\,(=c/\nu)$ such that

$$B_\lambda(T) = \frac{c_1}{\lambda^5(e^{c_2/k_B \lambda T} - 1)}, \tag{8.3}$$

where $c_1 = 1.191 \times 10^{-16}\,\mathrm{W\,m^{-2}\,sr^{-1}}$ and $c_2 = 1.4388 \times 10^{-2}\,\mathrm{m\,K}$. The Planck function defines the emitted monochromatic intensity for a given frequency (or wavelength) and temperature of the emitting substance. Recall that intensity, or radiance, is the radiant power per unit solid angle (steradian) and implies directionality in the radiation stream. Blackbody radiant energy increases with temperature, whereas the wavelength of maximum intensity λ_m decreases with increasing temperature $(\lambda_m = a/T$, where T is temperature in K and a is a constant). This relationship between the wavelength of maximum intensity and temperature is called Wien's displacement law. Note that the two curves of emitted monochromatic intensity in Fig. 8.1 are determined directly from (8.3), while the decrease in the wavelength of maximum intensity with temperature can be seen from Wien's displacement law.

A solid angle, $d\Omega$, as used in the definition of radiance, or intensity, is a surface area on a unit sphere (defined to have radius of 1). The equation for a solid angle is

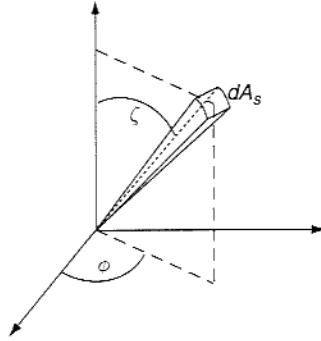$$d\Omega = \frac{dA_s}{r^2}, \tag{8.4}$$

Figure 8.3. An illustration of a solid angle as defined using polar coordinates. A pencil of radiation extends from the center of a sphere through area dA_s.

where dA_s is the surface area on a sphere of radius r (Fig. 8.3). Solid angles have units of steradians, which are analogous to the use of radians for a circle. The surface area dA_s is found to be

$$dA_s = (r \, d\zeta)[r \sin(\zeta) \, d\phi] = r^2 \sin(\zeta) \, d\zeta \, d\phi, \tag{8.5}$$

where ζ and ϕ are the zenith and azimuth angles, respectively. Thus, we have

$$d\Omega = \frac{dA_s}{r^2} = \sin(\zeta) \, d\zeta \, d\phi. \tag{8.6}$$

If this equation is integrated over an entire hemisphere, then

$$\Omega_h = \int_0^{2\pi} \int_0^{\pi/2} \sin(\zeta) \, d\zeta \, d\phi = 2\pi \text{ steradians.} \tag{8.7}$$

Now, if the amount of radiance passing through a given horizontal plane parallel to the Earth's surface is desired, then the component of radiation normal to this surface is needed. Knowledge of the zenith angle definition allows us to define this normal component as

$$F_\lambda = I_\lambda \cos(\zeta), \tag{8.8}$$

where I_λ is the intensity, or radiance, for a given wavelength. If this relationship is integrated over an entire hemisphere, then

$$F = \int_0^{2\pi} \int_0^{\pi/2} I_\lambda \cos(\zeta) \sin(\zeta) \, d\zeta \, d\phi, \tag{8.9}$$

and if the emitted radiation is isotropic, then this expression further simplifies to

$$F = I_\lambda \int_0^{2\pi} \int_0^{\pi/2} \cos(\zeta)\sin(\zeta)\, d\zeta\, d\phi = \pi I_\lambda. \qquad (8.10)$$

If the Planck function is similarly integrated over all frequencies/wavelengths, and all directions within a hemisphere, and it is assumed that the emitted radiation is isotropic, then one finds that

$$F = \pi B(T) = \sigma T^4. \qquad (8.11)$$

This is the well-known Stefan–Boltzmann law, where σ is the Stefan Boltzmann constant ($\sigma = 5.67 \times 10^{-8}\,\mathrm{W\,m^{-2}\,K^{-4}}$). This expression represents the maximum amount of radiative energy that an object can emit at a given temperature. Since this quantity is integrated over an entire hemisphere of directions, it represents the irradiance. In general, the irradiance depends upon the orientation of the surface.

8.2.2 Radiative transfer

As a pencil of radiation traverses a layer in the atmosphere, it will be weakened by its interaction with various atmospheric constituents (Fig. 8.4). The decrease in the intensity I_λ of the radiation at wavelength λ is observed to follow

$$dI_\lambda = -k_\lambda \rho I_\lambda\, ds, \qquad (8.12)$$

where ρ is the density of the gas, k_λ is the absorption coefficient for radiation of wavelength λ (which is a measure of the fraction of gas molecules that are absorbing radiation at λ), and ds is the thickness of the layer.

We can integrate this equation to obtain the intensity I_λ after traversing a distance s in the absorbing material, yielding

$$I_\lambda(s) = I_\lambda(0)e^{-\int_0^s k_\lambda \rho\, ds}, \qquad (8.13)$$
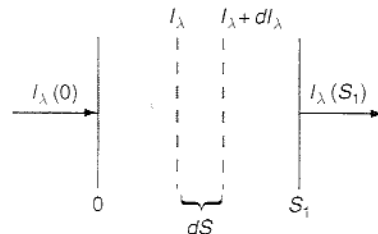

Figure 8.4. Depletion of the radiant intensity I_λ as it traverses an absorbing medium. After Liou (1980) reprinted with permission from Elsevier.

where $I_\lambda(0)$ is the intensity of the radiation at wavelength λ upon entering the atmospheric layer in question, and $I_\lambda(s)$ is the intensity upon exiting this layer. This relation is known as Beer's law, or the Beer–Bouguer–Lambert law in Liou (1980). This expression is often rewritten as

$$I_\lambda(s) = I_\lambda(0)e^{-\tau_\lambda}. \tag{8.14}$$

where

$$\tau_\lambda = \int_0^s k_\lambda \rho \, ds. \tag{8.15}$$

is called the optical depth, or optical thickness, depending upon the context (Liou 1980). The optical depth is a measure of the cumulative depletion that a beam of radiation experiences as it passes through a given layer.

Geometry also plays a role in calculating the optical depth used in models. It is convenient to measure the distance normal to the surface of the Earth, yet the direction of radiation is often at some angle to this upwardly directed normal. This angle is again our good friend the zenith angle. As the zenith angle increases from zero, a beam of radiation passes through more and more gas molecules as it traverses across a given layer of thickness dz. Thus, to change the integral defining the optical depth from ds to dz, we need to take into account the zenith angle. This leads to

$$\tau_\lambda = \frac{1}{\cos \zeta} \int_{z_1}^{z_2} k_\lambda \rho \, dz. \tag{8.16}$$

For any electromagnetic radiation I_λ that passes through a medium, such as the atmosphere, some of the energy is absorbed, some is scattered, and some is transmitted through the medium. Thus, the conservation of energy requires that

$$\frac{I_\lambda(\text{absorbed})}{I_\lambda} + \frac{I_\lambda(\text{reflected})}{I_\lambda} + \frac{I_\lambda(\text{transmitted})}{I_\lambda} = a_\lambda + r_\lambda + t_\lambda = 1, \tag{8.17}$$

where a_λ is the monochromatic absorptivity, r_λ is the monochromatic reflectivity, and t_λ is the monochromatic transmissivity. When a_λ is non-zero, then one also has to incorporate the emission of radiation from the medium through which the radiation is passing. This yields, following Liou (1980), the relationship

$$\frac{dI_\lambda}{k_\lambda \rho \, ds} = -I_\lambda + B_\lambda(T) + J_\lambda, \tag{8.18}$$

where T is the absolute temperature of the medium, $-I_\lambda$ represents the loss of radiance from attenuation (absorption plus scattering), $B_\lambda(T)$ represents the emission of radiance from the medium, and J_λ represents a second source of radiation from scattering into the line segment ds.

For longwave radiation, the scattering of radiation is negligible (Liou 1980), yielding the simplified equation of radiative transfer

$$\frac{dI_\lambda}{k_\lambda \rho \, ds} = -I_\lambda + B_\lambda(T). \tag{8.19}$$

If we assume a plane-parallel atmosphere (i.e., the atmosphere varies much more in the vertical than the horizontal direction and that the Earth is large enough to be considered flat) and account for the orientation of the radiation beam to the upwardly pointing normal, and use our definition of the optical depth from[1] τ, where $d\tau_\lambda = -k_\lambda \rho \, ds$, then we find that the equation of radiative transfer becomes

$$-\frac{dI_\lambda}{d\tau_\lambda \cos \zeta^{-1}} = -I_\lambda + B_\lambda(T). \tag{8.20}$$

Solutions commonly are found separately for upward and downward radiances. The general procedure to obtain a solution is to multiply the equation by the integrating factor $e^{-\tau_\lambda / \cos \zeta}$ and to integrate over the layer. After combining the two I_λ terms on the left-hand side, the equation becomes

$$-\int_{z_1}^{z_2} d\left[I_\lambda(z) e^{-\tau_\lambda(z)/\cos\zeta}\right] = \int_{z_1}^{z_2} B_\lambda(T) e^{-\tau_\lambda(z)/\cos\zeta} \, d\tau_\lambda. \tag{8.21}$$

If we then integrate the left-hand side term from z_1 to z_2 and divide both sides by $e^{-\tau_\lambda(z_2)/\cos\zeta}$ we find that after rearrangement we are left with

$$I_\lambda(z_2) = I_\lambda(z_1) e^{-[\tau_\lambda(z_1)-\tau_\lambda(z_2)]/\cos\zeta} + \int_{z_1}^{z_2} B_\lambda(T) e^{-[\tau_\lambda(z_1)-\tau_\lambda(z_2)]/\cos\zeta} \, d\tau_\lambda. \tag{8.22}$$

The first term on the right-hand side again represents the attenuation of the outgoing radiation, while the second term is the internal atmospheric contribution over the layer (Liou 1980).

Since the shortwave and longwave portions of the spectral distributions of irradiance are distinct, we can develop separate parameterizations for each component. We begin with discussions of the longwave component, since this is the one that is most expensive computationally.

---

[1] Optical depth increases in the opposite sense to z, and hence the negative sign.

8.3 Longwave radiative flux

8.3.1 Empirical methods

As discussed earlier, there are two basic approaches to the parameterization of radiation that have been used in models. The simplest and least computationally demanding, but likely to be the least accurate, is an empirical approach that relates bulk properties to the radiative flux. For example, numerous methods have been developed to estimate the downwelling longwave radiation at the ground from surface observations (Monteith and Unsworth 1990). One of the simplest approaches is to assume

$$Q_{Ld} = c + d\sigma T_a^4, \tag{8.23}$$

where c and d are constants calculated from observations and T_a is the 2 m air temperature. Unsworth and Monteith (1975) find that $c = -119 \pm 16\,\mathrm{W\,m^{-2}}$ and $d = 1.06 \pm 0.04$, using observations from the English Midlands. Similar values are determined over Australia by Swinbank (1968). Extensions to these types of statistical correlations of radiative fluxes with weather variables are possible for cloud conditions as well (Unsworth and Monteith 1975). They are most accurate under average weather conditions and are not appropriate for use at all times and places.

A similar approach is used by Anthes *et al.* (1987) to calculate the net longwave radiation at the surface, where they define

$$Q_{L_{net}} = \varepsilon_g \varepsilon_a \sigma T_a^4 - \varepsilon_g \sigma T_g^4. \tag{8.24}$$

Here T_g is the ground temperature (K), T_a is the air temperature approximately 40 hPa above the ground surface, ε_g is the ground or soil emissivity (typically 0.9–1.0), σ is the Stefan–Boltzmann constant, and ε_a is the atmospheric longwave emissivity. The downward longwave component is based upon the work of Monteith (1961) who shows that

$$\varepsilon_a = 0.725 + 0.17 \log_{10} w_p, \tag{8.25}$$

in which w_p is the total column precipitable water in centimeters. While computationally very efficient, these empirical approaches provide no information on the radiative flux divergence above the ground that can be dynamically important to cloud formation and breakup. In general, these approaches also neglect gaseous emissions from sources other than water vapor.

When clouds are present, the approach of Anthes *et al.* (1987) simply increases the downwelling longwave component using an enhancement factor, such that

$$Q_{Ld} = Q_{Ld_{clear}} \left(1 + \sum_{i=1}^{3} c_i n_i \right), \tag{8.26}$$

where n_i is the cloud fraction for a given atmospheric layer (low, middle, high), and the c_i values are given by

Cloud level	c_i
Low ($i = 1$)	0.26
Middle ($i = 2$)	0.22
High ($i = 3$)	0.06

The cloud layers are typically defined based upon the maximum relative humidity between specified pressure levels. The influences of clouds on radiation are discussed more fully in the following chapter on cloud cover.

8.3.2 *Two-stream methods for clear skies*

The other approach to parameterizing the longwave radiative flux is based upon solving the radiative transfer equation as discussed by Liou (1980). The discussion in this section is largely based upon Stephens (1984) and Ellingston *et al.* (1991). The equations appropriate for longwave flux are

$$F_U(z) = \int_0^{\infty} \pi B_\nu(0) \tau_\nu^f(z,0) \, d\nu + \int_0^{\infty} \int_0^z \pi B_\nu(z') \frac{d\tau_\nu^f}{dz'}(z,z') \, dz' \, d\nu, \tag{8.27}$$

$$F_D(z) = \int_0^{\infty} \int_z^{\infty} \pi B_\nu(z') \frac{d\tau_\nu^f}{dz'}(z,z') \, dz' \, d\nu, \tag{8.28}$$

where F_U and F_D are the upward and downward fluxes through height z, B_ν is the Planck function, and τ_ν^f is the diffuse transmission function defined over a hemisphere. The first term in F_U represents the attenuation of the longwave radiation emitted from the Earth's surface, while the second term represents the emittance of longwave radiation by the atmosphere. The single term in F_D represents the atmospheric contributions only. The diffuse transmission function is written as

$$\tau_\nu^f(z,z') = 2 \int_0^1 \tau_\nu(z,z',\mu) \, \mu \, d\mu. \tag{8.29}$$

where[2] $\mu = \cos(\zeta)$ and

$$\tau_\nu(z, z', \mu) = \exp\left[-\frac{1}{\mu}\int_{u(z)}^{u(z')} k_\nu(p, T)\, du\right], \tag{8.30}$$

in which $k_\nu(p, T)$ is the absorption coefficient (a function of pressure p and temperature T) and u is the concentration of the attenuating gas along the path from z to z'. The different parameterizations for longwave radiation differ in how these four integrals are calculated, owing to the need to minimize the computational costs. However, several common assumptions are found within these schemes.

The first common assumption is that one can replace the integration over all zenith angles in the $\tau_\nu^f(z, z')$ equation with the simplification

$$\tau_\nu^f(z, z') \propto \tau_\nu(z, z', 1/\beta), \tag{8.31}$$

where β is the diffusivity factor and is equal to 1.66. This states that the transmission of flux through the slab from z to z' is equivalent to the transmission of a beam along the zenith angle $\zeta = \cos^{-1}(1/\beta)$. This has been found to be a very reasonable and useful approximation (Rodgers and Walshaw 1966; Liu and Schmetz 1988).

The second group of common assumptions involves the integration of the absorption coefficient over the optical path. While it is known that k_ν is a function of p and T, laboratory data used to calculate k_ν are determined using constant values of p and T instead of the rapid changes observed in the atmosphere. Two common approximations used to determine $\tau_\nu(z, z', \mu)$, the scaling and the two-parameter approximation, both assume that absorption along a non-homogeneous path can be approximated by absorption along a homogeneous path using adjusted values of p and T.

The scaling approximation assumes that the absorption coefficient depends only upon the value of k_ν at reference p and T and the concentration of the attenuating gas u. Thus, the scaling approximation assumes

$$k_\nu(p, T) = k_\nu(p_0, T_0)\tilde{u} = k_\nu(p_0, T_0)\int_{u(z)}^{u(z')}\left(\frac{p}{p_0}\right)^n\left(\frac{T_0}{T}\right)^m du, \tag{8.32}$$

where m and n are constants that are specified for various absorbing species and range from 0 to 1.75 for n and from 0 to 11 for m. The variable $\tilde{u}$ is the adjusted concentration of the attenuating gas u. The variables p_0 and T_0 are the

---

[2] In radiative transfer discussions, this polar angle is measured relative to a beam pointing upwards, so $\zeta = 0$ and $\mu = 1$ for a beam pointing upwards, and $\zeta = \pi$ and $\mu = -1$ for a beam pointing downwards.

reference pressure and temperature. Goody (1964) provides further informa-
tion on this approximation.

The two-parameter approximation was proposed by Curtis (1952), Godson
(1954), and Van de Hulst (1945) and so is often called the VCG approximation.
It allows for more accurate approximations of the path integral by using two
parameters to relate the absorption along a non-homogeneous path to that of
a corresponding homogeneous path. It assumes that the mean transmission
between two levels is the same as if all the absorbing gas along the path were at
a constant pressure (Rodgers and Walshaw 1966). Thus, it adjusts both the
path u and the pressure p according to

$$
\begin{aligned}
\tilde{p}\tilde{u} &= \int p \, du \\
\tilde{u} &= \int du.
\end{aligned}
\tag{8.33}
$$

This adjustment is found by matching the absorption in the strong and weak
limits. Thus, instead of the path integral only depending upon the absorber
concentration as in the scaling approximation, it now depends upon both the
absorber concentration and the mean pressure.

A third method also has come into use recently. Instead of scaling a refer-
ence set of k_ν values as a function of u and p, a third method linearly
interpolates between stored sets of k_ν values that have been previously calcu-
lated over the full range of atmospheric conditions. The generation of these
stored sets of k_ν values is a significant overhead cost, and requires the use of
a very computationally expensive line-by-line radiative transfer model.
Presently, this approach is used only in the rapid radiative transfer model
(RRTM) as discussed in Mlawer *et al.* (1997).

Now that we have approximations that allow for easy calculation of the
transmissivity function, the integrations over frequency remain. This is where
the differences in the parameterizations are more clearly seen. The problem of
integrating over frequency is more complex than simply averaging k_ν over
some interval $\Delta\nu$. As illustrated by Stephens (1984), there are four distinguish-
able frequency scales that must be taken into account when making this
calculation. These scales range from the smoothly varying Planck function
to the rapidly varying absorption lines for the different absorbers (Fig. 8.5). As
discussed by Liou (1980), the examination of high-resolution spectroscopy
shows that the emissions of certain gases are composed of a large number of
characteristic spectral lines. These lines occur because each quantum jump
between fixed energy levels within an electron results in emission or absorption
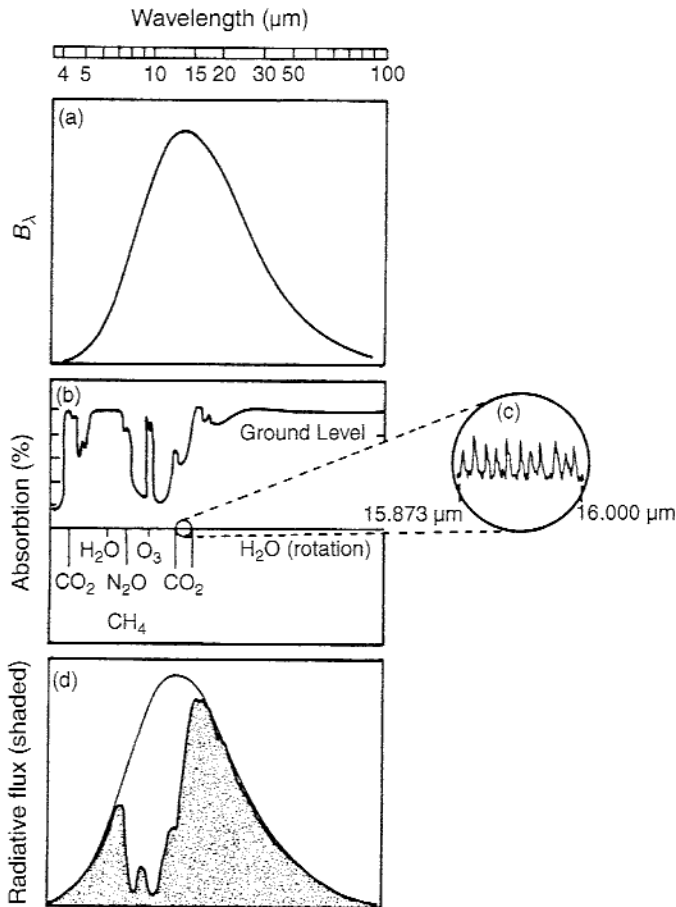
Wavelength (µm)

Figure 8.5. Schematic diagram illustrating the different frequency scales involved in the calculation of atmospheric longwave flux. These frequency scales are (a) the Planck curve, (b) atmospheric gaseous absorption spectrum for longwave radiation reaching the ground surface, (c) the individual absorption lines and line separations found when looking at very small frequency intervals, and (d) the convolution of the Planck function and the atmospheric absorption spectrum to give the atmospheric longwave flux (shaded area). From Stephens (1984).

of a characteristic frequency, which then appear as absorption lines. Two general parameterization approaches are used to surmount the challenges provided by these widely varying functions included in the frequency integration. The first approach is to divide the Planck function into a number of discrete intervals, define the absorption characteristics of each interval separately, and sum the resulting values (narrow-band models). The second method is to convolve the absorption and Planck functions and integrate

this quantity over large portions of the longwave spectrum (wide-band models). We begin by looking at the narrow-band models.

8.3.3 Narrow-band models

Band models use average absorption properties for bands of lines that are specified by well-defined statistical relationships. The resulting transmission functions are defined as (Stephens 1984)

$$\tau_\nu = \exp\left[\frac{-\bar{S}u\beta}{\bar{d}}\left(1 + \frac{\bar{S}u\beta}{\pi\bar{\alpha}}\right)^{-1/2}\right]. \qquad (8.34)$$

where the overbar represents an average over $\Delta\nu$. $\bar{S}$ is a mean line intensity, $\bar{\alpha}$ is a mean line half-width, $\bar{d}$ is a mean line spacing, and β is the diffusivity factor. The various values of $\bar{S}/\bar{d}$, and $\pi\bar{\alpha}/\bar{d}$ for the two water vapor bands, the 15 μm CO_2 band, the 9.6 μm O_3 band, and the 6.3 μm water vapor vibration band are found in Rodgers and Walshaw (1966), Goldman and Kyle (1968), and Wu (1980). One requirement of band models is that the Planck function must be treated as a constant across the frequency interval selected, often leading to the need for narrow frequency bands. It is also limited by the behavior of the transmission function, which does not take an exponential form across broad spectral bands. While Rodgers and Walshaw (1966) used only 21 intervals to span the longwave absorption spectrum, the computational efforts required are still very expensive for operational considerations. Morcrette and Fouquart (1985) use over 300 bands to explore systematic errors in longwave radiation calculations.

An alternative approach to the narrow-band method that is demonstrably faster and more accurate is the correlated-k, or k-distribution, method. This method uses the fact that the transmission within a relatively wide spectral interval is independent of the ordering of the values of the absorption coefficient k_ν with respect to ν. Thus, for an assumed homogeneous atmosphere, the transmission depends on the fraction of the selected interval $f(k)$ that is associated with a particular value of k. This approach groups frequency intervals according to line strengths, and the transmission function is rewritten as

$$\tau_{\bar{\nu}}(z, z') = \frac{1}{\Delta\nu}\int_{\Delta\nu} e^{-k_\nu u}\,d\nu = \int_0^\infty f(k)e^{-ku}\,dk. \qquad (8.35)$$

Thus, instead of integrating over frequency, one integrates over the absorption coefficient values (Fig. 8.6). Errors associated with the correlated-k technique
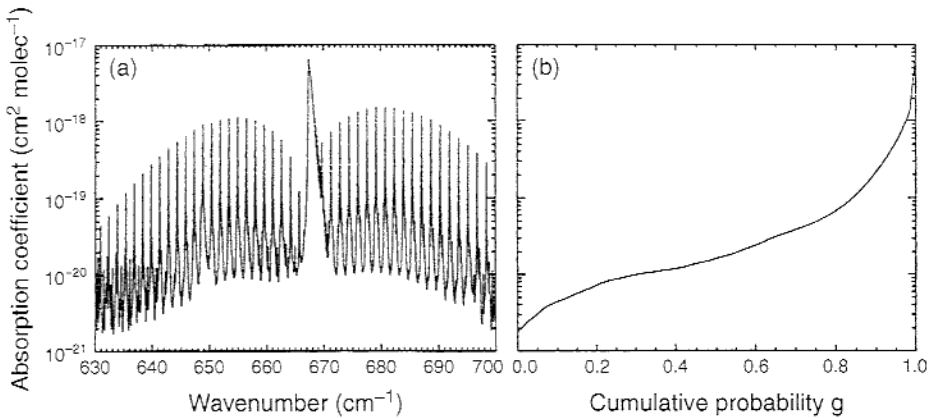
Figure 8.6. Absorption coefficients due to carbon dioxide for a layer at 507 hPa in the middle of summer (a) as a function of wavenumber, and (b) after being rearranged in ascending order for the spectra range 630–700 cm^{-1}. From Mlawer *et al.* (1997).

are at least a factor of two smaller than most other band models, and the technique is computationally faster as well. Lacis and Oinas (1991) suggest that the correlated-k technique produces results to within 1% of a line-by-line radiative transfer model (LBLRTM), while Fu and Liou (1992) explore the mathematical and physical conditions under which the method is valid and find that it works well for atmospheric radiative transfer. Differences in cooling rates between the rapid radiative transfer model (RRTM), which uses this approach, and a LBLRTM are typically less than 0.15 K day^{-1} for clear skies (Mlawer *et al.* 1997).

The main differences between the various narrow-band models are the number of frequency bands used in the calculations, whether the scaling or two-parameter approximation is used for the optical path integration, and the data sets used to generate the transmission functions for the spectral intervals. However, other details can also be important. As pointed out by Stephens (1984), while the absorption in the "atmospheric window" between 8 and 14 μm is weak, it is important to reproduce it accurately as significant amounts of radiant energy are exchanged between the ground surface, clouds, and space. Another concern is the method by which the transmission of two different gases that absorb radiation in the same spectral interval (e.g., H_2O and CO_2) is handled. Please refer to Stephens (1984) and Ellingston *et al.* (1991) for further discussions and details on these narrow-band methods. In addition, Edwards and Slingo (1996) develop a two-stream radiation parameterization in which the spectral resolution of the code is variable, allowing

for one to evaluate the sensitivity of radiative transfer calculations to changes in the parameterizations of the physical processes.

8.3.4 Wide-band models (emissivity models)

Narrow-band models are limited by the need to define a frequency interval that is narrow enough that the Planck function can be treated as a constant across the interval. In addition, the transmission function is no longer exponential across broad intervals, further limiting the width of the bands that can be used and thereby increasing the computational cost. A function that largely overcomes these limitations is emissivity, the ratio of the power emitted by a body at a given temperature T to the power emitted if the same body obeyed Planck's law.

Emissivity ε is thus defined as

$$\varepsilon(z, z') = \frac{1}{\sigma T^4} \int_0^\infty A_\nu(z, z') \pi B_\nu(T) \, d\nu, \tag{8.36}$$

where $A_\nu (= 1 - \tau_0)$ is the absorptivity of the gas. This allows us to rewrite the radiative flux equation following Stephens (1984) as

$$F_U(z) = \sigma T_g^4 (1 - \varepsilon(z, 0)) + \int_0^z \sigma T^4(z') \frac{d\varepsilon}{dz'}(z, z') \, dz', \tag{8.37}$$

$$F_D(z) = \int_z^\infty \sigma T^4(z') \frac{d\varepsilon}{dz'}(z, z') \, dz'. \tag{8.38}$$

Note that the integration over frequency has now vanished from the radiative flux equations! Emissivity has physical significance and can be measured, although there is a fair amount of ambiguity in these measurements when gas emissions overlap. However, the solution of these flux equations is easy given the emissivity as a function of the absorber concentration u (Charlock and Herman 1976; Sasamori 1968; Staley and Jurica 1970).

As an example, Rodgers (1967) develops an upward and downward emissivity as

$$\varepsilon(u) = \sum_{n=0}^N b_n (\ln(u))^n, \tag{8.39}$$

where u is the water vapor path and b_n are constants that depend upon temperature. For u less than $10 \, \mathrm{g\,m^{-2}}$, an alternative expression is used such that

$$\varepsilon(u) = \sum_{n=1}^{N} a_n u^{n/2}, \tag{8.40}$$

where a_n are constants that depend upon temperature. The variable N is the number of terms in the polynomial expansion and equals 4 in Rodgers (1967). This approach is used by Dudhia (1989) in a mesoscale weather prediction model.

One challenge to the broad-band method is that it is not always simple to obtain expressions of emissivity as a function of absorber concentration u that are sufficiently accurate to obtain precise values of $d\varepsilon/du$ or $d\varepsilon/dz$. If instead a modified emissivity is defined as

$$\varepsilon'(z, z') = \int_0^\infty A_\nu(z, z') \frac{dB_\nu(T)}{d\sigma T^4(z')} \, d\nu = \frac{R(z, z')}{4\sigma T^3}, \tag{8.41}$$

where $R(z, z')$ is the mean absorptivity parameter (Elsasser and Culbertson 1960), then an integration by parts of the original emissivity form of the flux equation yields

$$F_U(z) = \sigma T_g^4 + \int_0^z \varepsilon'(z, z') \frac{d\sigma \, T^4(z')}{dz'} \, dz', \tag{8.42}$$

$$F_D(z) = \int_z^\infty \varepsilon'(z, z') \frac{d\sigma \, T^4(z')}{dz'} \, dz'. \tag{8.43}$$

While ε' is not directly related to ε, it also doesn't greatly differ from ε. Indeed, Ramanathan *et al.* (1983) define the relationship

$$\varepsilon = \frac{\varepsilon'}{0.847u^{0.222}}, \tag{8.44}$$

where u is the absorber concentration, which allows us to convert from one emissivity to the other. Rodgers (1967) shows that the flux calculations are most accurate when ε' is used to calculate F_U and ε is used to calculate F_D.

Another widely used emissivity-based approach is the simplified exchange method (SEM) of Fels and Schwarzkopf (1975) and Schwarzkopf and Fels (1991). This method recognizes that, in many situations, the dominant contribution to atmospheric cooling rates at any given height is from the "cool-to-space" (CTS) term (Fig. 8.7) as discussed by Rodgers and Walshaw (1966). The total cooling rate Q can then be divided into two parts
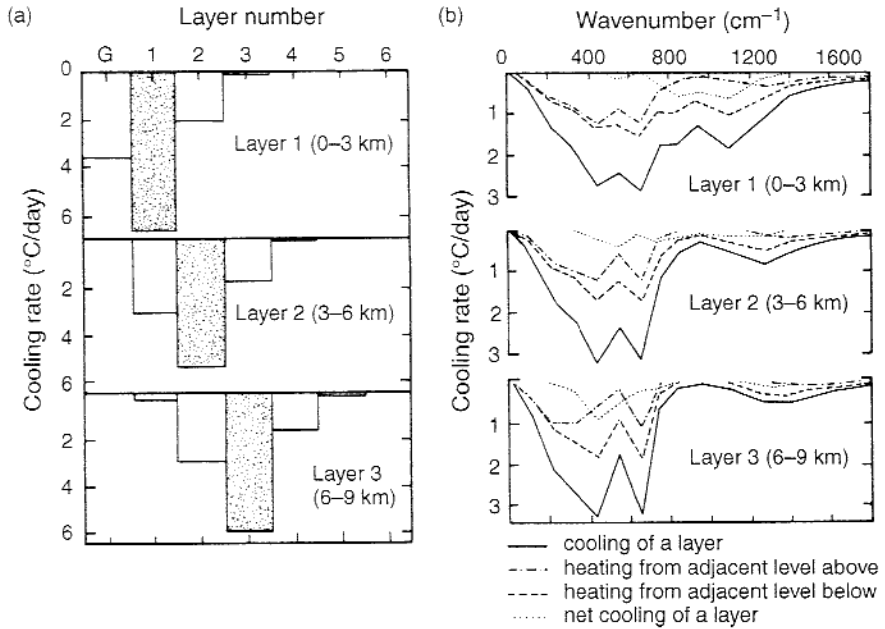
$$Q = Q_{ex} + Q_{CTS}, \tag{8.45}$$

Figure 8.7. The contribution to the specified 3 km deep layer longwave radiative cooling from the layer itself (shaded) and the absorption of longwave radiation from adjacent 3 km deep layers (left). Shaded areas denote cooling, whereas the open areas denote warming from the adjacent layers. Also shown is the spectral distribution of the cooling/heating for the three 3 km deep layers (right). Cooling to space is the largest contribution in each of the three layers shown. From Stephens (1984) as modified from Wu (1980).

where Q_{ex} is the exchange term and Q_{CTS} is the cool-to-space term. Since Q_{CTS} is the dominant term, it needs to be calculated very accurately. In contrast, Q_{ex} can be calculated using approximate techniques with little loss of accuracy. This division of the calculation into accurate and approximate approaches is the key characteristic of this approach (Fig. 8.8). Thus, one can calculate Q_{ex} using

$$Q_{ex} = Q^\epsilon - Q^\epsilon_{CTS}, \qquad (8.46)$$

where both Q^ϵ and Q^ϵ_{CTS} are determined using broad-band emissivity methods. The Q_{CTS} term is calculated using

$$\frac{\partial T}{\partial t} = \frac{g}{c_p} \sum_n B_n(T) \frac{\partial \bar{\tau}_n}{\partial p}(0,p), \qquad (8.47)$$

for an isothermal atmosphere at temperature T, where n is the number of frequency bands. This equation is used to determine the cooling rates at every
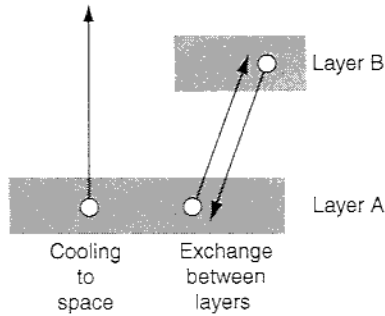
Figure 8.8. Schematic diagram of the two different contributions to the radiative cooling of a layer in the atmosphere. One contribution is the cooling to space, which occurs mainly in the transparent regions of the absorption spectrum. The other contribution is by mutual exchange between layers, say layers A and B, as illustrated. After Stephens (1984).

level in the model, even when T is not constant. The computational efficiency of this CTS term compared to other emissivity methods is that the cooling rates are a function of T and only depend upon the absorber concentration above the level in question. Thus, the CTS term is calculated using multiple bands, while the broad-band emissivity method is used for the exchange term. This yields computational efficiency and accurate calculations.

The above discussion outlines various approaches to longwave radiative flux calculations that apply to any given layer of the atmosphere. To incorporate these equations into a numerical weather prediction model, the values of F_U and F_D are calculated at each vertical model level. Then the heating rate is calculated from the flux divergence between every two vertical levels using a finite-difference form. Stephens (1984) suggests that around a dozen or so vertical levels are needed for relatively accurate calculations if there are no significant discontinuities in moisture or temperature in the vertical direction. But computational efficiency is always a concern, leading to efforts to develop very fast radiation parameterizations (e.g., Harshvardhan *et al.* 1987).

Ellingston *et al.* (1991) discuss results from an international project to compare radiation codes used in climate models under clear-sky conditions. Fifty-five separate cases are used to compare the various methods, representing a range of conditions. Results indicate that the line-by-line models and the narrow-band models agree to about $\pm 2\%$ for fluxes at the atmospheric boundaries and to about $\pm 5\%$ for the flux divergence in the troposphere. However, only five wide-band models are found to match the performance of the narrow-band models. Many of the less detailed parameterizations display a spread of 10–20% in their calculations. However, many changes have occurred since 1991. First, the parameterizations have constantly evolved

over time, such that results with newer schemes should be an improvement over those shown by Ellingston *et al.* Second, the Atmospheric Radiation Measurement Program (Stokes and Schwartz 1994) has assisted in funding further refinements to radiation parameterizations and more detailed comparisons with observations.

8.4 Shortwave radiative flux

8.4.1 Empirical methods

As with longwave methods, the simplest of the shortwave radiation parameterization schemes only predict the total shortwave radiation that reaches the Earth's surface. These schemes do not incorporate the effects of shortwave absorption on atmospheric diabatic heating. They can be based upon detailed comparisons with more complex shortwave radiative transfer models, or upon comparisons with observations. Regardless of the specific approach, their main advantage is their computational efficiency.

Anthes *et al.* (1987) present a fairly typical approach to calculating the amount of shortwave radiation that reaches the surface. They approximate

$$Q_S = S_0(1 - a)\tau \cos(\zeta), \tag{8.48}$$

where S_0 is the solar constant, a is the albedo, ζ is the solar zenith angle, and τ is the shortwave transmissivity. This transmissivity term is based upon the work of Benjamin (1983) for multiple reflections and is defined as

$$\tau = \tau_a[\tau_s + (1 - \tau_s)(1 - b)]/(1 - X_R a), \tag{8.49}$$

where τ_a is the absorption transmissivity, τ_s is the scattering transmissivity, b is the backscatter coefficient, and X_R is the multiple reflection factor where

$$X_R = \tau_{ad}(1 - \tau_{sd})b_d. \tag{8.50}$$

The τ_{ad}, τ_{sd}, and b_d terms refer to absorption, scattering, and backscatter parameters for diffuse radiation. These clear-air transmissivities (τ_a, τ_s, τ_{ad}, τ_{sd}) are functions of path length and precipitable water as found from the Carlson and Boland (1978) radiative transfer model.

Benjamin (1983) also presents a scheme to alter the shortwave radiation based upon the amount of cloud cover. Three layers of cloud are allowed, depending upon the atmospheric pressure: low clouds for pressures greater than 800 hPa, middle clouds for pressures between 800 and 450 hPa, and high clouds for pressures below 450 hPa. He then defines

Table 8.1. *Values of absorption and scattering transmissivity parameters for determining the total transmissivity when clouds are present from Benjamin (1983).*

Cloud level	τ_{ai}	τ_{si}
Low ($i=1$)	0.80	0.48
Middle ($i=2$)	0.85	0.60
High ($i=3$)	0.98	0.80

$$\tau_{ac} = \prod_{i=1}^{3} [1 - (1 - \tau_{ai})]n_i, \tag{8.51}$$

$$\tau_{sc} = \prod_{i=1}^{3} [1 - (1 - \tau_{si})]n_i, \tag{8.52}$$

where n_i is the cloud fraction (0 to 1) for each of the cloud layers and is based upon the maximum relative humidity value in each layer, and the absorption transmissivities for each layer are predetermined and shown in Table 8.1. The total transmissivity for a cloudy atmosphere is then defined by

$$\tau = \frac{\tau_{ac}\tau_{sc}\tau_a[\tau_s + (1 - \tau_s)(1 - b)]}{1 - X_C a}, \tag{8.53}$$

where

$$X_C = \tau_{ad}\tau_{ac}(1 - \tau_{sd}\tau_{sc})\overline{b_d}, \tag{8.54}$$

and

$$\overline{b_d} = \frac{b_d(1 - \tau_{sd}) + (1 - \tau_{sc})}{(1 - \tau_{sd}) + (1 - \tau_{sc})}. \tag{8.55}$$

It should be noted that applying fixed, predetermined shortwave characteristics to clouds is problematic. The radiative properties of clouds change with the changing cloud character and with zenith angle. Thus, determining just what values for transmissivity should be used is not clear and these approaches without doubt do not work well in all circumstances.

Savijärvi (1990) presents a slightly more detailed approach for clear skies, defining

$$Q_S = S_0 \sin(h)\left[1 - 0.024(\sin(h))^{-0.5} - 0.11aa(u/\sin(h))^{0.25}\right.$$
$$\left. - as(0.28/(1 + 6.43\sin(h)) - 0.07a)\right], \tag{8.56}$$

where

$$u = \int_{p_{sfc}}^{0} q\left(\frac{p}{1013}\right)^{0.85}\left(\frac{273}{T}\right)^{0.5}\frac{dp}{g} \tag{8.57}$$

is a scaling approximation that represents a linearly pressure-scaled vertical water vapor amount (cm), and h is the local hour angle of the sun. This equation accounts for O_3, H_2O, and CO_2 depletion as well as Rayleigh scattering. The parameters aa and as (both ≥ 1) represent a crude inclusion of aerosol absorption and scattering, respectively. Savijärvi suggests that the best results are found with $aa = 1.2$ and $as = 1.25$ for continental industrialized areas.

Unlike the Anthes et al. approach. Savijärvi also includes a simple parameterization for solar heating in the atmosphere, using

$$\frac{\partial T}{\partial t} = S_0\left(\frac{q}{c_p}\right)\left(\frac{p}{p_0}\right)\left[y\frac{u}{\sin(h)} + 1.67ay(u_*)\sin(h)\right] + 1.7 \times 10^{-6}[\sin(h)]^{0.3}, \tag{8.58}$$

where u_* is u calculated from the surface to the top of the atmosphere, and

$$y = \begin{cases} 0.029u^{-0.81} & u \geq 0.05 \text{ cm} \\ 0.050u^{-0.63} & u < 0.05 \text{ cm}. \end{cases} \tag{8.59}$$

The Atwater and Ball (1981) constant cloud transmission functions are recommended when clouds are present.

Finally, the last example for the empirical approaches is from Dudhia (1989), who provides a slightly more complex one-stream approach. He defines

$$F_D(z) = \mu S_0 - \int_{z}^{\infty} (dS_{cs} + dS_{ca} + dS_s + dS_a), \tag{8.60}$$

where S_{cs} and S_{ca} are the decreases in irradiance from cloud scattering and absorption, and S_s and S_a are the decreases in irradiance from clear-air scattering and absorption. The parameterization assumes that the cloud fraction is either 0 (no cloud) or 1 (overcast) for each grid point.

The scattering and absorption coefficient values are bilinearly interpolated from Stephens' (1978b) tabulated functions of μ and the natural logarithm of

the liquid water path for cloudy conditions and from the Lacis and Hansen (1974) absorption function for clear-air conditions (which requires μ and the water vapor path). Dudhia indicates that the total effect of a cloud layer above a height z is obtained from the above function as a percentage of the downward solar flux that is absorbed or reflected by clouds. Then at height $z - \Delta z$, a new total percentage is determined that incorporates the absorption and scattering effects of the layer Δz. Thus, the clear-air effect above z is removed since clouds are present. Clear-air scattering is assumed to be uniform and proportional to the atmospheric mass path length, allowing for zenith angle effects, with 10% scattering occurring in one atmosphere. The atmospheric heating rate is computed from the vertical change in the absorption terms.

8.4.2 Two-stream methods in clear skies

The parameterization of shortwave radiative flux has many similarities to the parameterizations for longwave radiative flux discussed previously. However, instead of being grouped into general types (narrow-band, broad-band), the schemes are named (Eddington, delta-Eddington, quadrature, hemispheric, two-stream) based upon the choices made in approximating the effective zenith angle for the stream directions and how and when the single-scattering phase function is approximated. This definitely lends a different flavor to the literature.

Unlike longwave radiation, both absorption and scattering are important processes for shortwave radiation and need to be included. Stephens (1984) indicates that Rayleigh scatter is dominant only for the shorter wavelengths, while liquid water absorption in clouds occurs only for the longer wavelengths, leading to a natural division on either side of the $0.7\,\mu m$ wavelength. The transfer of shortwave radiation is not as complex as longwave radiation, since the problem of the simultaneous absorption and emission of radiation from layer to layer does not occur. Thus, although not as computationally demanding as longwave schemes, shortwave schemes still require substantial computer time and approximations are needed to produce schemes that can run within operational models.

Following the discussions of Stephens (1984) and Pincus and Ackermann (2003), the shortwave irradiance is often separated into direct (*dir*) and diffuse (*dif*) components, where the direct component represents the contributions from photons that have not been scattered. Thus,

$$I(\tau, \mu, \varphi) = I_{dir}(\tau, \mu, \varphi) + I_{dif}(\tau, \mu, \varphi). \tag{8.61}$$

The direct component follows Beer's law, such that the irradiance reaching a given level z is given by

$$F_D(z, \mu_0) = \mu_0 \int_0^\infty S_\nu(\infty) \tau_\nu(z, \infty, \mu_0) \, d\nu, \tag{8.62}$$

where

$$\tau_\nu(z, \infty, \mu_0) = \exp\left(-\frac{1}{\mu_0} \int_z^\infty k_\nu \, du\right). \tag{8.63}$$

While problems similar to those found in calculating longwave radiation are present in the path and frequency integrals, the values of $S_\nu(\infty)$ are known and specified a priori. One can use a narrow- or broad-band approach to calculate the integral. The correlated-k, or k-distribution, method also can be used to improve the accuracy and speed of the calculations for shortwave radiation.

In addition, Stephens (1984) indicates that the effects of pressure and temperature on k_ν are only a complication for water vapor absorption. Thus, if desired, one can define a mean transmission function

$$\tau_{\bar\nu}(z, \infty, \mu_0) = \frac{1}{\Delta\nu} \int_{\Delta\nu} \exp\left(-m_r(\mu_0) \int_z^\infty k_\nu \, du\right) d\nu, \tag{8.64}$$

where $m_r(\mu_0)$ is a relative air mass factor and differs from $1/\mu_0$ only at large zenith angles greater than 75° (and for ozone – see Rodgers 1967). This could be considered a broad-band approach.

With these assumptions one can then rewrite the integral over frequency as a summation and obtain

$$F_D(z) = \mu_0 \sum_{i=1}^N S_i(\infty) \tau_{\bar\nu i}(u), \tag{8.65}$$

where N is the number of frequency intervals and u is the absorber path length from z to ∞ along the zenith angle.

Since the direct component of radiation follows Beer's law, and therefore is relatively easy to code, most of the literature describes the ways in which the diffuse component of shortwave radiation is handled. The azimuthally averaged monochromatic radiative transfer equation for a given frequency ν is

$$\mu \frac{dI}{d\tau} = -I(\tau, \mu) + \frac{\omega_0}{2} \int_{-1}^1 \bar p(\tau, \mu, \mu') I(\tau, \mu') \, d\mu' + \frac{\omega_0 S_0}{4\pi} \bar p(\tau, \mu, \mu_0) e^{-\tau/\mu_0},$$

$$\tag{8.66}$$

where ω_0 is the single-scattering albedo, which is the likelihood that a photon is scattered rather than absorbed at each interaction (and varies from 0 to 1), $\bar{p}$ is the scattering phase function that characterizes the angular distribution of the scattered radiation field, S_0 is the solar constant (W m^{-2}), and μ_0 is the cosine of the zenith angle of the sun as always. To obtain the irradiance, this equation must be integrated over frequency and zenith angle. The first term on the right-hand side is the diffuse radiation that enters into the layer in question. The second term represents the increase in diffuse radiation from multiple scattering, while the last term represents the increase in diffuse radiation from single scattering of direct solar radiation. Thus, it is easy to see how scattering complicates the calculations. In addition, since the intensity I appears on both sides of the equation, this an integrodifferential equation which is quite difficult to solve.

The optical thickness τ now includes contributions from scattering and absorption. The scattering phase function $\bar{p}$ describes how likely it is that radiation traveling in the (μ', ϕ') direction will be scattered, by molecules or cloud droplets, into the (μ, ϕ) direction. The value of a phase function can vary over several orders of magnitude as the scattering angle is varied and illustrates complex behavior. Analytic formulas are used to approximate the phase function and can be compared against a full Rayleigh or Mie scattering calculation for accuracy. Thankfully, the exact nature of the scattering phase function is not incredibly important, as multiple scatter tends to smooth out its peaks when hemispheric integrals are calculated. This is a key point, since the full scattering calculations show a great deal of structure in the scattering phase function. Yet it is clear that the scattering phase function approximation used does make a difference in the accuracy of the results.

The phase function can be described in terms of a scattering angle Θ between the incident and scattered radiation from a frame of reference centered on a particle. A useful parameter to use in describing the phase function is the asymmetry parameter g, such that

$$g = \frac{1}{2} \int_{-1}^{1} \cos \Theta \; \bar{p}(\Theta) \; d\cos \Theta, \qquad (8.67)$$

which varies from -1 for complete backscatter, to 0 for isotropic scatter, to $+1$ for complete forward scatter.

8.4.3 Eddington approach

As discussed earlier, the schemes are named based upon the choices made in approximating the various terms in the integrals for the shortwave radiation

flux. The Eddington approximation as discussed by Pincus and Ackermann (2003) uses an expansion for both intensity and phase to first order, such that each varies linearly with μ as

$$I(\mu) = I_0 + I_1\mu$$
$$\bar{p}(\tau, \mu, \mu_0) = 1 + 3g\mu\mu'. \tag{8.68}$$

This yields for the diffuse radiative transfer equation, after evaluating the integral and rearranging some terms,

$$\mu\frac{dI_0}{d\tau} + \mu^2\frac{dI_1}{d\tau} = I_0(1 - \omega_0) + I_1\mu(1 - \omega_0 g) - \frac{\omega_0}{4}(1 - 3g\mu\mu_0)S_0 e^{-\tau/\mu_0}. \tag{8.69}$$

A pair of equations for I_0 and I_1 are obtained by first integrating over μ from -1 to 1 and then multiplying by μ and again conducting this same integration. This yields

$$\frac{dI_0}{d\tau} = (1 - \omega_0 g)I_1 + \frac{3\omega_0}{4\pi}g\mu_0 S_0 e^{-\tau/\mu_0}, \tag{8.70}$$

$$\frac{dI_1}{d\tau} = 3(1 - \omega_0)I_0 - \frac{3\omega_0}{4\pi}S_0 e^{-\tau/\mu_0}. \tag{8.71}$$

These two first-order equations in I_0 and I_1 can be solved, following Shettle and Weinman (1970), providing solutions that are a sum of exponentials in τ, such as

$$I_0 = Ae^{k\tau} + Be^{-k\tau} + \phi e^{-\tau/\mu_0}, \tag{8.72}$$

where A, B, and ϕ are determined from the boundary conditions at the top and bottom of the atmosphere and from the particular solution.

The diffuse irradiances (fluxes) are then computed from I_0 and I_1 using

$$F_D(\tau, \omega_0, g, \mu_0) = 2\pi\int_0^1 (I_0 + \mu I_1)\mu\, d\mu = \pi\left(I_0 + \frac{2}{3}I_1\right), \tag{8.73}$$

$$F_U(\tau, \omega_0, g, \mu_0) = 2\pi\int_0^1 (I_0 + \mu I_1)\mu\, d\mu = \pi\left(I_0 - \frac{2}{3}I_1\right). \tag{8.74}$$

Since different frequencies are associated with different parameter values for ω_0, g, and τ, these expressions for F_D and F_U must be integrated over all frequencies to get the total diffuse irradiance.

8.4.4 Delta-Eddington approach

The Eddington approximation is not as accurate as many would like, and particularly has problems in optically thin atmospheres and when large absorption is involved, so Joseph *et al.* (1976) develop a modification to the phase function that performs better. The original phase function approximation, which contains a large and narrow forward peak in scattering, is replaced with a delta function in the forward direction and a smoother scaled phase function elsewhere. This results in a new approximation for the phase function, such that

$$\bar{p}(\cos\Theta) \approx 2f\partial(1 - \cos\Theta) + (1-f)(1 + 3g'\cos\Theta), \qquad (8.75)$$

where f is the fractional scattering into the forward peak, ∂ is the Dirac delta function, and g' is the asymmetry factor of the truncated phase function (Pincus and Ackermann 2003). Joseph *et al.* (1976) require that this phase function have the same asymmetry factor (g) as the original phase function, which defines a specific relationship between g' and g. They also define $f = g^2$. When all the equations are derived, it is seen that this approach just rescales the original Eddington solutions.

One application of the delta-Eddington approach is discussed by Briegleb (1992). In this parameterization, originally developed for the NCAR Community Climate Model version 2 (CCM2), the solar spectrum is divided into 18 bands. Seven bands are for O_3, one band for the visible, seven bands are for H_2O, and the final three bands are for CO_2. The model atmosphere consists of a discrete set of horizontally homogeneous layers. The delta-Eddington solution consists of evaluating the solution for the reflectivity and transmissivity of each layer, and then combining the layers together to obtain the upward and downward spectral fluxes. This is repeated for all 18 spectral bands to accumulate broad-band fluxes, from which heating rates then can be calculated.

8.4.5 Two-stream approach

While the terminology is a little bit confusing, there is another method to solve the radiative transfer equation that is called the two-stream method (Liou

1980). This should not be confused with the general idea that most methods used to solve the radiative transfer equation consist of calculating two streams of radiation: one in the upward direction and one in the downward direction. This "two-stream" method is just one particular approach to solving the same problem. While the Eddington approach expands the intensity and phase into first order in angle, the two-stream model first averages the radiative transfer equation and phase function over each hemisphere to obtain the radiative flux, and then computes the solution. Thus, the azimuthally averaged radiative transfer equation is integrated over the hemisphere to obtain the upward and downward fluxes, leading to two separate equations

$$\bar{\mu}\frac{dF_D}{d\tau} = F_D - \omega_0(1-b)F_D + \omega_0 b F_U - \frac{\omega_0}{2\pi}[1-b(\mu_0)]S_0 e^{-\tau/\mu_0}, \quad (8.76)$$

$$\bar{\mu}\frac{dF_U}{d\tau} = F_U - \omega_0(1-b)F_U + \omega_0 b F_D - \frac{\omega_0}{2\pi}b(\mu_0)S_0 e^{-\tau/\mu_0}, \quad (8.77)$$

where b is the backscattering coefficient (Pincus and Ackermann 2003). These are two first-order, linear coupled differential equations with constant coefficients. The solutions are found by uncoupling the equations through differentiating with respect to optical thickness, and then substituting the other equation. The solutions end up being a sum of exponentials in optical thickness, just as found for the Eddington solutions.

All two-stream methods can be generalized to a generic form, where

$$\frac{dF_U}{d\tau} = \gamma_1 F_U - \gamma_2 F_D + \frac{S_0}{4}\tilde{\omega}_0\gamma_3 e^{-\tau/\mu_0}, \quad (8.78)$$

$$\frac{dF_D}{d\tau} = \gamma_2 F_U - \gamma_1 F_D + \frac{S_0}{4}\tilde{\omega}_0\gamma_4 e^{-\tau/\mu_0}, \quad (8.79)$$

provided that an explicit assumption is made regarding the dependence of I upon μ. Values of reflectance R and transmittance T can be derived directly from these equations. The heart of these two-stream approaches is a suitable choice of τ, $\tilde{\omega}_0$, and g for each spectral interval and absorber. Note that the heating from CO_2 and O_2 absorption lines is usually added to the heating by water vapor absorption, since the contributions of both CO_2 and O_2 to solar heating are small (Stephens 1984). Meador and Weaver (1980) derive the various formulas for numerous two-stream approaches and discuss the different assumptions that go into their development.

The above discussion outlines several approaches to shortwave radiative flux calculations that apply to any given layer of the atmosphere. To incorporate these equations into a numerical weather prediction model, the values of F_U and F_D again need to be calculated at each vertical model level just as is done for the longwave flux. However, this is more complicated than the calculations for longwave flux, owing to the effects of multiple scattering that must be taken into account. The two-stream solutions discussed above apply to a single homogeneous layer with fixed values of τ, $\tilde{\omega}_0$, and g, and so the challenge is to combine several layers with these varying optical properties. Several different techniques are available that can be used for this purpose.

The adding method is one approach to calculating the shortwave radiative flux across multiple vertical levels. Take two adjacent vertical layers in the atmosphere. The upper layer has transmittance T_1 and reflectance R_1, while the lower layer has transmittance T_2 and reflectance R_2. To find out how much total flux is reflected from this combination of layers, we examine the multiple reflections. First, some of the flux that enters the upper layer is reflected immediately (R_1). However, some is also transmitted through the layer, is reflected by the lower layer, and then transmitted back through the first layer ($T_1 R_2 T_1$). Some of this flux is reflected back from the upper layer and again reflected back from the lower layer, finally passing through the upper layer ($T_1 R_2 R_1 R_2 T_1$). This process goes on and on (Pincus and Ackermann 2003), yielding

$$
\begin{aligned}
R_T &= R_1 + T_1 R_2 T_1 + T_1 R_2 R_1 R_2 T_1 + T_1 R_2 R_1 R_2 R_1 R_2 T_1 + \cdots \\
R_T &= R_1 + T_1 R_2 [1 + R_1 R_2]^{-1} T_1.
\end{aligned}
\tag{8.80}
$$

This equation for total reflectance is combined with its analog for transmittance with the delta-Eddington or other two-stream models to compute the transmittance and reflectance of layered atmospheres. The adding–doubling method extends this general approach to intensity (Pincus and Ackermann 2003). Stephens (1984) illustrates that an equivalent approach is to consider the atmosphere as a system of n homogeneous layers with specified values for reflectance and transmission. This allows one to construct an equivalent linear system of $3n + 3$ equations, the solution of which produces the equivalent adding algorithm. Pincus and Ackermann (2003) also discuss an eigenvector approach termed the discrete ordinate approach.

8.5 Radiative transfer data sets

Numerical weather prediction models provide the vertical profiles of temperature, pressure, and water vapor mixing ratio needed for longwave and

shortwave radiative transfer calculations under clear skies, but gas and particle concentrations also are needed in these calculations. Of the gases important to radiative transfer calculations, carbon dioxide and oxygen are considered permanent constituents of the atmosphere and have nearly constant volume ratios up to 60 km (Liou 1980). Although the concentration of carbon dioxide does vary slightly throughout the annual cycle (variations of $\sim$6 parts per million (ppm) by volume with a concentration of $\sim$375 ppm in 2004), it also has been increasing throughout the years owing to the burning of fossil fuels and these changes are estimated for use in global climate models. In contrast, ozone is more variable in time and space, although it typically resides at levels between 15–30 km above ground. This variability requires that the ozone distribution be specified in the numerical model through reference to typical distributions (e.g. London *et al.* 1976). Total column ozone concentration also can be observed by satellite (Heath *et al.* 1975), but the radiative transfer calculations still need the vertical distribution. Jang *et al.* (2003) suggest that this can be estimated from vertical mean potential vorticity and show that the inclusion of real-time ozone data into a numerical weather prediction model can lead to improvements in forecasts. At present, operational models generally use an ozone climatology.

Finally, aerosols are important to shortwave absorption and scattering. Aerosols can scatter and absorb shortwave radiation, thereby changing the diffuse fraction of the shortwave radiative flux and influencing the terrestrial carbon cycle (Niyogi *et al.* 2004). In addition, aerosols can act as condensation nuclei for cloud droplets, thereby enhancing the amount of cloud cover, and influencing cloud lifetimes and precipitation efficiencies (Twomey 1977; Albrecht 1989). Some aerosols are created by natural processes, such as from sea spray, dust, smoke from natural forest fires, chemical reactions, boreal forests, and volcanic eruptions. Other aerosols are produced by humankind as a consequence of fuel combustion and are often commonly referred to as pollution. Obviously aerosols also can vary greatly in time and space. In general, aerosol concentrations in the troposphere are much greater than those in the stratosphere, except after volcanic eruptions. Tropospheric aerosols have lifetimes of several days, emphasizing their variability. Most models presently use typical aerosol distributions in the radiative transfer calculations, while developers are moving to include real-time total column aerosol concentrations based upon satellite data in combination with information from climatology or surface aerosol observing networks such as the Aerosol Robotic Network (AERONET; Dubovik and King 2000) to provide the distributions needed for radiative transfer calculations (see King *et al.* 1999; Al-Saadi *et al.* 2005).

8.6 Discussion

Relatively sophisticated and computationally affordable radiative transfer parameterizations have been developed for both the shortwave and longwave radiation components. These schemes provide the net surface radiation for the land surface schemes, which is partitioned into the total available energy for sensible, latent, and ground heat fluxes, and the vertical radiative flux divergence, which is used to calculate the radiative heating and cooling rates of a given atmospheric volume. Errors in the net radiation clearly influence these surface flux amounts and feed back to influence boundary layer structure and depth (Guichard *et al.* 2003; Zamora *et al.* 2003), and eventually even cloud development and precipitation. Thus, accurate radiation parameterizations are very important to the success of numerical weather prediction.

Comparisons of present operational and research models with observations generally indicate that the predicted amounts of surface incoming shortwave radiation are too large (Fig. 8.9) (Betts *et al.* 1997; Halthore *et al.* 1998; Hinkelman *et al.* 1999; Chevallier and Morcrette 2000; Barker *et al.* 2003; Marshall *et al.* 2003; Zamora *et al.* 2003). This high bias is probably due to
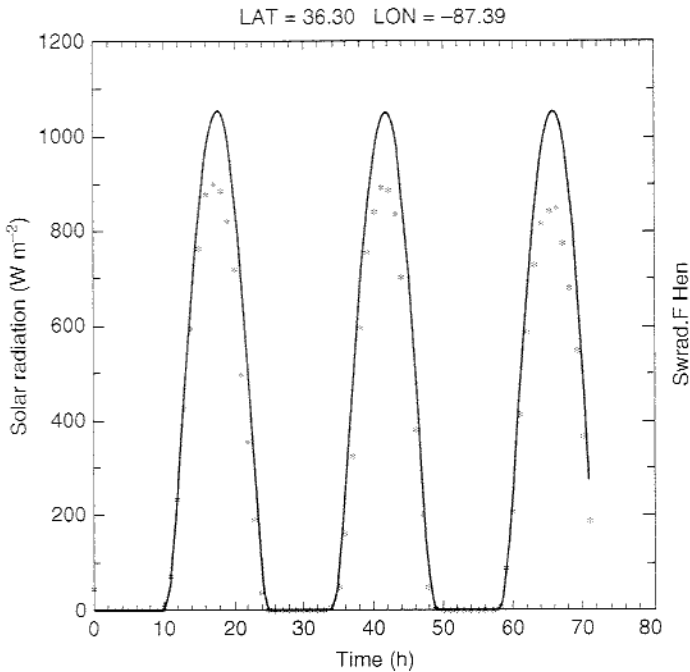

Figure 8.9. Total solar flux predicted by a numerical model (solid line) and measured at New Hendersonville, Tennessee (asterisks) between 11 and 14 June 1995. From Zamora *et al.* (2003).

either the lack of a combination of aerosol and ozone absorption (Zamora *et al.* 2003) or to excessive simplifications in the shortwave radiation parameterization (Morcrette 2002). When the aerosol optical depths and amounts of ozone are known, then Satheesh *et al.* (1999), Mlawer *et al.* (2000), and Zamora *et al.* (2003) indicate good agreement between the predicted and observed amount of surface shortwave radiation. Satheesh *et al.* (1999) show that the total shortwave flux decreases by 50–80 W m^{-2} when including aerosol radiative forcing based upon observed aerosol characteristics, with similar results from Zamora *et al.* (2005) (Fig. 8.10). Zamora *et al.* (2003) further
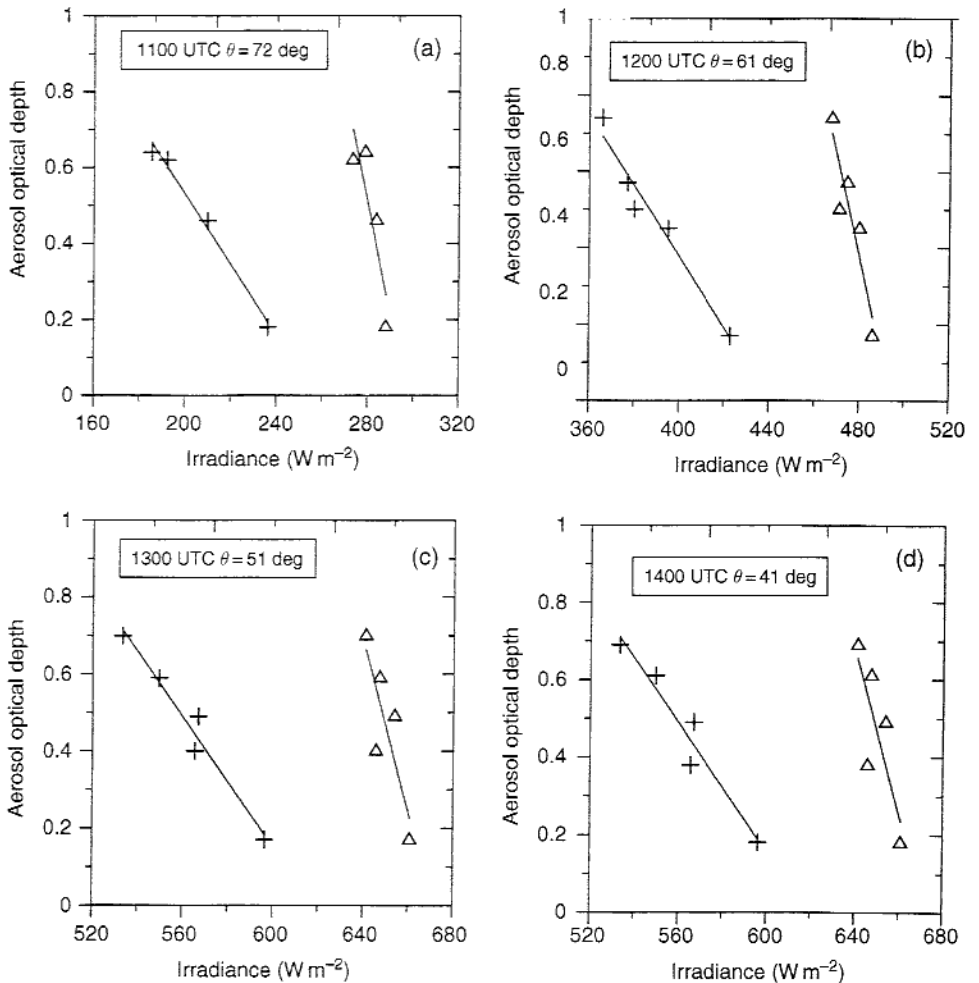

Figure 8.10. Correlation between aerosol optical depth and the observed (crosses) and Eta model (triangles) solar irradiances for zenith angles of (a) 72°, (b) 61°, (c) 51°, and (d) 41°, measured on five different cloud-free days during August 2002. From Zamora *et al.* (2005).
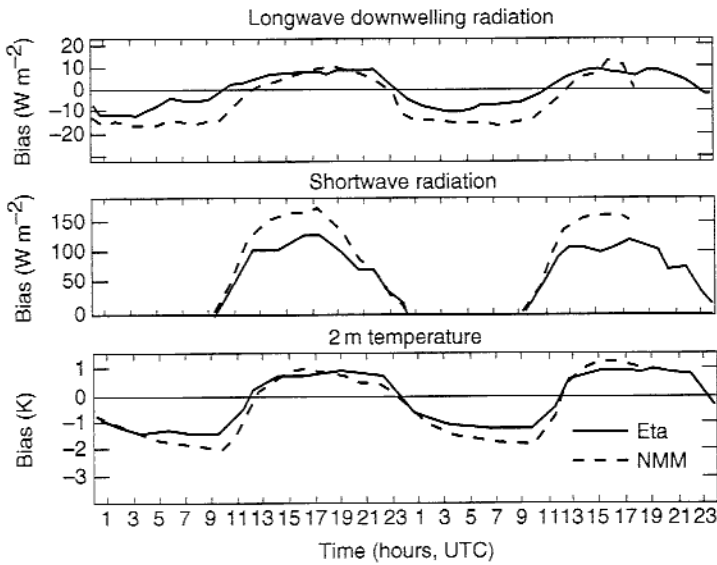
Figure 8.11. Plots of bias (model − observed) in downward longwave radiation (top), shortwave radiation (middle), and 2 m temperature (bottom) versus time (UTC) over the 48 h forecast time and averaged over 77 days. The models are the NCEP Eta model and the Non-hydrostatic Mesoscale Model (NMM). The downward longwave radiation was only observed at a single site (Plymouth, Massachusetts), whereas the solar radiation and the 2 m temperature are averages from six sites. After Stensrud *et al.* (2006).

show that stratospheric ozone alone can reduce the surface shortwave radiation by 20–30 W m^{-2}. The excessive net radiation at the surface leads to predicted daytime temperatures that are too warm (Fig. 8.11) and boundary layers that are too deep when compared with observations (Zamora *et al.* 2003).

Unfortunately, aerosol optical depths vary across a large range, from 0.02 to 0.4, and are influenced strongly by both natural and anthropogenic sources (sea salt from the oceans, mineral dust from arid land regions, sulfate and nitrate from both natural and anthropogenic sources, and organic and carbonaceous particles from burning (Satheesh *et al.* 1999)). Satheesh *et al.* (1999) show daily variations approaching 0.2 in aerosol optical depths over the Maldive Islands (Fig. 8.12). Yet aerosol optical depth is not commonly measured, reported, and ingested into models as part of our routine observational system, although this may soon change (King *et al.* 1999).

Intercomparisons of shortwave radiation parameterizations also have been undertaken and results summarized by Fouquart *et al.* (1991) and Boucher *et al.* (1998). As reported in Fouquart *et al.* (1991), even for the simplest case of pure water vapor absorption, root-mean-square (rms) differences of 1–3%
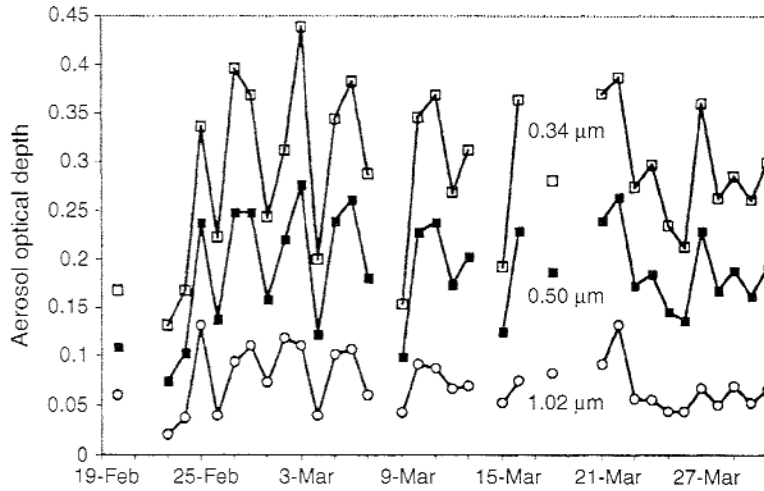
Figure 8.12. Daily mean aerosol optical depths for three representative wavelengths sampled over slightly more than 1 month at Kaashidhoo, Maldives. From Satheesh *et al.* (1999).

($\sim 10\,\mathrm{W\,m^{-2}}$) are found for the downward flux at the surface, with larger differences of 6–11% for the total atmospheric absorption. The rms differences in downward flux at the surface increase to 4% for low elevation angles. When aerosols and/or clouds are considered, the rms differences increase even further, with clouds producing differences of up to 10% ($50\,\mathrm{W\,m^{-2}}$) and aerosols up to 21% ($90\,\mathrm{W\,m^{-2}}$). Fouquart *et al.* (1991) note two main causes of the uncertainty in the shortwave calculations. First, the calculation of water vapor absorption is critical, yet large differences exist in the various parameterizations. Fundamental inadequacies may be associated with details in the spectral lines and/or irradiances at the top of the atmosphere. Second, that the interactions between multiple scattering and molecular absorption are very difficult to handle adequately with low spectral resolution methods. This is the cause of the large rms differences when aerosols or clouds are present. Boucher *et al.* (1998) compare the direct shortwave radiative forcing by sulfate aerosols in 15 different parameterizations and find a standard deviation of the zenith-angle-averaged normalized broad-band shortwave forcing of 8%, with somewhat larger standard deviations at some zenith angles. Most of the one-dimensional parameterizations overpredict surface shortwave radiation by 15–25 W m^{-2} at overhead sun for a standard tropical atmosphere, regardless of cloud cover. However, recent results by Bush *et al.* (2000), Dutton *et al.* (2001), and Philipona (2002) suggest that much of this presumed overprediction actually may be due to an underestimation of the observed clear-sky global and diffuse solar irradiance caused by pyranometer differential cooling
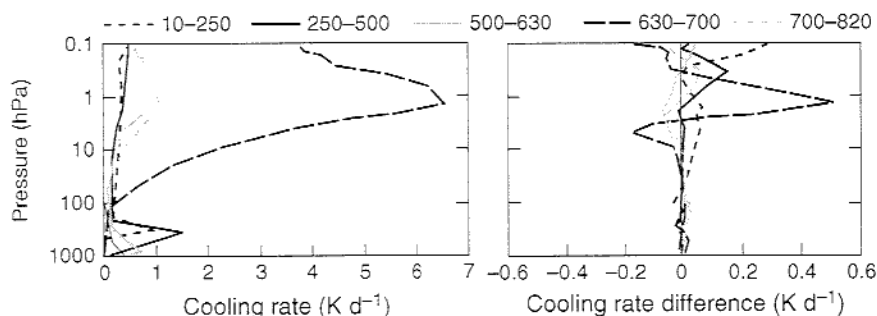
Figure 8.13. Spectrally integrated cooling rates (K day^{-1}) for each of the bands 1 through 5 (10–820 cm^{-1} as indicated in the figure) calculated by the line-by-line radiative transfer model (LBLRTM), and cooling rate differences (K day^{-1}) between RRTM and LBLRTM. Note that the cooling rate differences generally are less than 0.2 K day^{-1} and the flux differences are typically less than 0.6 W m^{-2} (not shown). After Mlawer et al. (1997).

when adequate ventilation and heating systems are not used. Philipona (2002) concludes that since most pyranometers in use worldwide do not have adequate ventilation and heating systems, archived global and diffuse radiation measurements largely are underestimated.

For longwave radiation parameterizations, the results are more mixed. Mlawer et al. (1997) show good agreement between the RRTM and a line-by-line radiative transfer model (Fig. 8.13), while Zamora et al. (2003) show good agreement between surface incoming longwave radiation from the RRTM and observations. However, a broad-band emissivity parameterization does not fare as well in the comparison as it overpredicts the mean incoming radiation by 80 W m^{-2} (Zamora et al. 2003). This overprediction leads to the model being unable to develop a nocturnal stable boundary layer and a low-level jet. Comparisons of present operational models from the USA with observations over the New England region (Stensrud et al. 2006) show that the model parameterizations underpredict the incoming longwave radiation by 10–20 W m^{-2}, leading to surface nighttime temperatures that are too cool (Fig. 8.11). Similar results are found in Hinkelman et al. (1999).

The terrain slope, orientation, and sky view also influence the amount of radiation received at the surface. Avissar and Pielke (1989) illustrate the importance that terrain slope and orientation can have on the incoming solar radiation, yet these effects are not always incorporated into models. A parameterization that includes the effects of terrain on both longwave and shortwave radiation is developed by Müller and Scherer (2005) and yields smaller 2 m air temperature errors in comparison with simulations that do not include the terrain effects.

Radiation parameterizations

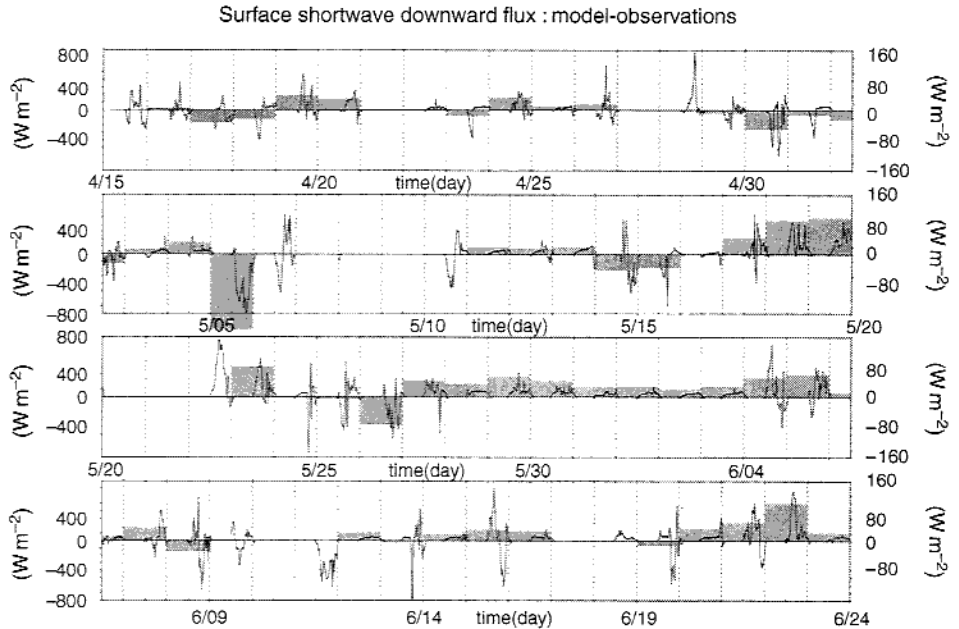Surface shortwave downward flux : model-observations

Figure 8.14. Time series of surface downward shortwave radiation differences (simulated – observed) for 15 April through 24 June 1998 over the Atmospheric Radiation Measurement Southern Great Plains site in Lamont, Oklahoma. Values are 30 minute averages. Gray shading denotes the mean daily values, using the axis on the right-hand side of the figure. From Guichard *et al.* (2003).

A comparison of amounts of surface radiation versus observations suggests that on short timescales the differences between the predicted and observed amounts can be quite large on a large number of days (Fig. 8.14). Differences of several hundred $W m^{-2}$ in incoming surface shortwave radiation and between 50 and 100 $W m^{-2}$ for incoming longwave radiation are not unusual. Undoubtedly, many of these differences are due to clouds, which are covered in the next chapter. While the daily average values of predicted radiation may be relatively close to the observations, these large short timescale differences make one wonder about how this inaccuracy in incoming surface radiation influences the model behavior. Is it good enough to get the daily average net radiation, or is it also important to get the instantaneous radiation amounts correct? This is an important question for numerical weather prediction and the answers may very well be case dependent. Certainly we have learned that small differences over even short time periods can be important when the weather situation is uncertain and a host of outcomes are possible. If this position is true, indicating that a high level of accuracy is needed in the instantaneous radiation fluxes, then we have a long way to go in developing

radiation parameterizations with the needed level of accuracy for use in numerical weather prediction models.

Finally, as the grid spacing in models continues to decrease, the validity of using model data from a single vertical column (i.e., the plane-parallel assumption) for radiative transfer calculations comes into question. Clearly as horizontal grid spacings approach 1 km the use of a single vertical column to describe the radiation transfer becomes fraught with difficulties, as radiation reaching a given location on the Earth's surface clearly passes through multiple horizontal grid cells. Monte Carlo photon transport codes are available that track individual photons in three dimensions from their entry points in a column to their exit points and allow photons to move from grid cell to grid cell (e.g., Marchuk *et al.* 1980; Barker and Davies 1992; Chylek and Dobbie 1995; Marshak and Davis 2005). Another approach for three-dimensional radiative transfer is the spherical harmonic discrete ordinate method (Evans 1998). Typically these methods are used in situations where the plane-parallel assumption is poor, such as when clouds are present, and are not used in operational models owing to their computational expense. These methods are summarized and plans for their development and testing outlined in Cahalan *et al.* (2005).

8.7 Questions

The basic ideas behind most of the radiative transfer parameterization schemes are similar, so let us examine the behavior and construction of one of the schemes. Lacis and Hansen (1974) examine how ozone and water vapor influence the total solar flux. The fraction of total solar flux absorbed in the lth layer of the atmosphere by ozone, where $l = 1$ is the top of the atmosphere and l increases downward, is defined as

$$A_l = \mu_0 \{ A(x_{l+1}) - A(x_l) + \overline{R}(\mu_0) [A(x_l^*) - A(x_{l+1}^*)] \}, \qquad (8.81)$$

where $\overline{R}(\mu_0)$ is the albedo of the reflecting region, x_l is the ozone path traversed by the direct solar beam in reaching the lth layer, and x_l^* is the ozone path of the diffuse radiation illuminating the lth layer from below. Ozone absorption is modeled as a purely absorbing region sitting on top of a purely reflecting region. For our purposes, all ozone is generally assumed to lie above the troposphere, or above approximately 100 hPa. The albedo of the reflecting region is defined as

$$\overline{R}(\mu_0) = \overline{R}a(\mu_0) + [1 - \overline{R}a(\mu_0)](1 - \overline{\overline{R}}a^*)Rg/(1 - \overline{\overline{R}}a^* Rg), \qquad (8.82)$$

where Rg is the ground albedo, $\overline{\overline{R}}a^* = 0.144$, and the effective albedo of the lower atmosphere is defined as

$$\overline{Ra}(\mu_0) = \frac{0.219}{1 + 0.816\mu_0}. \tag{8.83}$$

for clear skies. They also define $x_l = u_l M$, where u_l is the amount of ozone in a vertical column above the lth layer, and

$$M = \frac{35}{(1224\mu_0^2 + 1)^{1/2}}, \tag{8.84}$$

is the magnification factor (Rodgers 1967) to account for path slant and refraction. The ozone path traversed by the diffuse radiation illuminating the lth layer from below is defined as

$$x_l^* = u_t M + \overline{M}(u_t - u_l), \tag{8.85}$$

where u_t is the total ozone above the main reflecting layer (the ground for clear skies), and $\overline{M} = 1.9$ is the effective magnification factor for diffuse radiation.

Finally, the fraction of incident solar flux absorbed by the Chappius visible band is defined as

$$A(x_l) = \frac{0.02118x_l}{1 + 0.042x_l + 0.000323x_l^2}, \tag{8.86}$$

and the absorption of the ultraviolet region is defined as

$$A(x_l) = \frac{1.082x_l}{(1 + 138.6x_l)^{0.805}} + \frac{0.0658x_l}{1 + (103.6x_l)^3}, \tag{8.87}$$

where the total absorption by ozone in the lth layer is the sum of the individual absorptions from the visible and ultraviolet regions.

If we assume a single layer of ozone above the troposphere with an ozone path x_2 above a single-scattering layer, then following Zamora *et al.* (2003) we find that

$$A = \mu_0 \{ A(x_2) + \overline{R}(\mu_0) [A[x_2(M + \overline{M})] - A[x_2 M]] \}. \tag{8.88}$$

1. Calculate the absorption of ozone for a zenith angle of $60°$ and for ozone path $x_2 = 0.2$, 0.3, 0.4, 0.5, and 0.6. Assuming a solar constant of $1368\,\mathrm{W\,m^{-2}}$ and a ground albedo $Rg = 0.10$, how much does the presence of ozone decrease the incoming solar radiation?

2. Now let us turn our attention to the absorption of solar radiation by water vapor. Lacis and Hansen (1974) discuss water vapor absorption further. One formula for water vapor absorption is

$$A(y) = \frac{2.9y}{(1 + 141.5y)^{0.635} + 5.925y},$$ (8.89)

where y is the precipitable water vapor in centimeters. The fractional absorption in the lth layer is then defined under clear skies as

$$A_l = \mu_0 \{ A(y_{l+1}) - A(y_l) + Rg[A(y_l^*) - A(y_{l+1}^*)] \},$$ (8.90)

where the effective amount of water vapor traversed by the direct solar beam is

$$y_l = \frac{M}{g} \int_0^{p_l} q \left(\frac{p}{p_0}\right)^n \left(\frac{T_0}{T}\right)^{1/2} dp,$$ (8.91)

in units of $kg\,m^{-2}$, and where the effective amount of water vapor traversed by the diffuse radiation reaching the lth layer from below is

$$y_l^* = \frac{M}{g} \int_0^{p_g} q \left(\frac{p}{p_0}\right)^n \left(\frac{T_0}{T}\right)^{1/2} dp + \frac{5}{3g} \int_{p_{l+1}}^{p_g} q \left(\frac{p}{p_0}\right)^n \left(\frac{T_0}{T}\right)^{1/2} dp,$$ (8.92)

where p_g is the ground pressure, g is the acceleration due to gravity, $p_0 = 1013$ mb, and $T_0 = 273.15$ K. One can convert y_l to units of cm by dividing by the density of water ($1000\,kg\,m^{-3}$) and multiplying by 100 to convert from m to cm. Assuming the atmospheric profile given below, calculate the heating rate in clear-sky conditions using $n = 0, 0.5$, and 1 to calculate the effective water vapor. Describe the influence of the pressure scaling on the resulting heating rates.

The sounding to use in calculating water vapor absorption is as follows.

p (mb)	T ($^\circ$C)	q ($g\,kg^{-1}$)
950.0	36.0	13.0
900.0	32.0	11.0
850.0	26.0	11.0
800.0	20.0	11.0
750.0	15.0	11.0
700.0	15.0	4.0
650.0	10.0	2.0
600.0	5.0	1.5
550.0	0.0	1.5
500.0	-8.0	1.0
450.0	-15.0	1.0
400.0	-20.0	0.4
350.0	-26.0	0.4
300.0	-30.0	0.4
250.0	-44.0	0.2
200.0	-53.0	0.1
150.0	-62.0	0.05
127.4	-67.0	0.05